Systematic process hazard assessment of three kinds of solid organic peroxides with kinetic analysis and heat transfer equilibrium

Shang-Hao Liu[1] · Yan-Ru Wang[1] · Chen-Rui Cao[1] · Yen-Chun Cheng[2]

Abstract
Organic peroxide (OP) has been applied in the industry for at least 40 years. Driven by significant investments in today's high-profile energy, petrochemical, and polymer industries, the market and applications of OPs are expanding rapidly. However, the self-reactive nature has led to continuous research work on this topic. Nevertheless, tremendous progress has been made in hazard analysis, which has improved existing protocols or led to the discovery of new safety methods. OPs still cause related chemical hazards, and the limitations related to process hazards remain to be resolved. There is a lack of comprehensive systematic analysis of the process hazards of a wide variety of OPs. Different OPs, namely BPO, LPO, and the emerging OP, HTP-65W, were selected for investigation with several calorimetry techniques based on thermokinetic and heat transfer models. Determination methods have a crucial role in an operator for obtaining a systematic understanding of hazard properties under different process conditions, which is related to avoiding the occurrence of process disasters. For example, LPO has a shorter TMR_{ad} and TCL (< 1 min) than BPO and HTP-65W, indicating that LPO can be classified as an obvious hazardous material. Moreover, $SADT < 25\ °C$ can be used for evaluating LPO's cooling system efficiency.

Keywords Organic peroxides · Self-reactive · Chemical hazard · Calorimetry · Hazardous material

List of symbols

A	Pre-exponential factor of the Arrhenius equation (s^{-1})
$A(\alpha)$	Pre-exponential factor at conversion (s^{-1})
$A'(\alpha)$	Amended pre-exponential factor by a product of $A(\alpha)$ and $f(\alpha)$ (s^{-1})
C_p	Specific heat capacity ($J\ g^{-1}\ K^{-1}$)
CT	Control temperature (°C)
E_a	Apparent activation energy ($kJ\ mol^{-1}$)
$E(\alpha)$	Apparent activation energy factor at conversion ($kJ\ mol^{-1}$)
ET	Emergency temperature (°C)
$f(\alpha)$	Kinetics function (dimensionless)
i	Component number (dimensionless)
n	Reaction order (dimensionless)
n_1, n_2	Reaction orders of a specific stage (dimensionless)
$Q\infty\,i$	Reaction calorific effect (W)
q	Heat flow rate (W)
R	Gas constant ($J\ mol^{-1}\ K^{-1}$)
r	Reaction rate constant ($mol\ L^{-1}\ s^{-1}$)
$SADT$	Self-accelerating decomposition temperature (°C)
t	Time (min)
T	Temperature of sample (K)
TCL	Time to conversion limit (day, hr or min)
T_0	Apparent exothermic onset temperature (°C)
TMR	Time to maximum rate (day)
TMR_{ad}	Time to maximum rate under adiabatic conditions (day)
TMR_{iso}	Time to maximum rate under isothermal conditions (day)
U	Heat transfer coefficient ($W\ m^{-2}\ K^{-1}$)
W	Heat generation ($J\ s^{-1}$)
x	Unit outer normal on the boundary (dimensionless)
z	Autocatalytic constant (dimensionless)
ΔH_d	Heat of decomposition ($J\ g^{-1}$)

✉ Shang-Hao Liu
shliu998@163.com

Chen-Rui Cao
harvettsao@foxmail.com

1 School of Chemical Engineering, Anhui University of Science and Technology, 168 Taifeng Street, Huainan 232001, Anhui, China

2 Shanghai Chemway Chemical Co., Ltd, Room 1208, Lane 408, Shitai Road, Baoshan District, Shanghai 200444, China

α	Degree conversion of a component (dimensionless)
β	Heating rate (°C min^{-1})
λ	Heat conductivity (W m^{-1} K^{-1})
ρ	Density (kg m^{-3})

Introduction

Historical development and application of organic peroxides in industrial fields

Industrial advancement and demand have also driven the applicability and researchability of traditional processes. Organic peroxide (OP) is a good example. Wind power generation [1], packaging of solar cells [2], and the development of renewable plastics [3, 4] have driven the demand for the polymerized plastics by OPs which have once again received numerous attention. According to the survey [5, 6], the OPs market continues to grow, and new production bases and capacity expansions are now underway. At the same time as industrial upgrading, it is a common phenomenon to increase storage to improve efficiency [5].

When OPs on process, storage, and transportation are exposed to high temperature or energy, electrons can be removed or added, leading to the homolytic cleavage of covalent bonds [7–11]. To show how this type of material undergoes decomposition, the phenomenon of the thermal decomposition of benzoyl peroxide (BPO) is shown in Fig. 1a, b as an example. The energy generated by breaking the bond in the OP initiator helps polymerization reactions overcome the activation energy barrier and proceed smoothly. The initiator monomer, which can act as a free radical initiator for polymerizations, also affects the quality of the polymerized product [12].

There are two ways to add the free radical formed by the initiator to the vinyl monomer. These two pathways are shown in Fig. 1c, d for the addition of an OP radical to a styrene monomer. However, the energy released by breaking the –O–O– bond can also cause heat to accumulate and increase the temperature and pressure in a closed process system such as a reactor. Continuing increases in temperature and pressure can eventually trigger fire and explosion hazards in the process [13].

The current situation and development of OPs explained by the perspective of the process industry

From a market survey report [14] based on Markets and Markets (M&M) Research Private Ltd., the global OP market was estimated at $902.4 million in 2017 and is expected to reach $1069.1 million by 2022, equaling a 3.4% compound annual growth rate. The overall performance of the market is driven by the increased demand for OPs in chemical and plastics applications. It is estimated that diacyl peroxides, such as BPO, lauroyl peroxide (LPO), and di-tert-butyl peroxyhexahydroterephthalate (HTP-65W), have the largest demand, which will elevate the growth trend in the global OP market in the near future.

In the industrial domain, in addition to its usage as a polymerization initiator, the pharmacological effects [15, 16] of BPO are gradually receiving attention. LPO is an essential ingredient for the production of plastics and rubber products, such as vinyl chloride, ethylene, styrene, and vinyl acetate [17]. HTP-65W can also be used for the polymerization of vinyl monomers. However, HTP-65W can polymerize monomers more efficiently than LPO because of its two
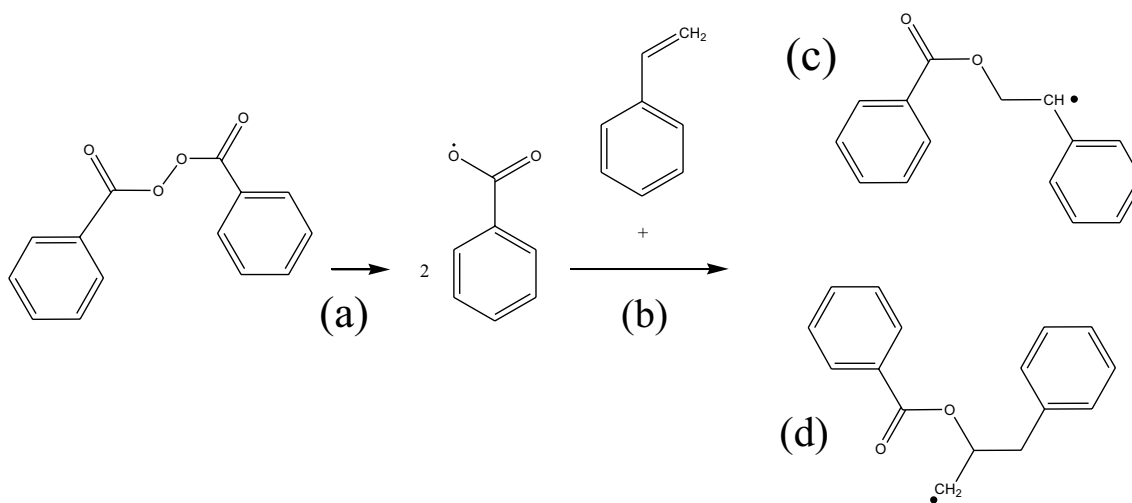

Fig. 1 Decomposition reaction mode of OPs in chemical processes: a case study of BPO [34]

O–O bonds, as can be observed from the chemical structures of LPO and HTP-65W shown in Fig. 2. These chemicals are widely used in areas including polymer modification, elastomer cross-linking, and maintenance. According to a report from AkzoNobel [18], OPs are also used in high-performance, polymer-insulated, high-voltage cables for improving power network technology and meeting the demand for connecting offshore wind power plants and other renewable energy sources, an application involved in the future support of sustainable energy. Even with advancements in industrial technology, OPs still occupy a place in the field of polymerization. This study selected an emerging OP, HTP-65W, and two classic OPs, BPO, and LPO, which are widely used for chemical polymerization but less for process safety-related research, such as investigations focused on industrial safety and hazard comparison.

The potential hazards and research status of OPs

According to the United Nations (UN) standards for categorization of hazardous materials, OPs are in class 5 hazardous category of materials. The UN (United Nations, 2018)

(United Nations, 2018) [19] and the Japan Fire and Disaster Management Agency classify OPs as dangerous goods with potential thermal hazard characteristics.

The hazardous properties of OPs are mainly characterized by the possibility of fire and explosive disaster, particularly self-reactive decomposition without oxygen that causes abundant heat release accompanied by the generation of gaseous products [20–23]. Even at ambient temperature, self-reactive OPs may cause heat accumulation and ultimately result in runaway reactions [7–9, 24, 25]. Thus, OP compounds have a specific self-reactive nature [26–29].

In the past, OPs [26, 29–32] have sporadically caused thermal hazards reflected by chemical accidents [30]. The most recent case of an accident happened in August 2017, when a severe explosion and fire occurred during the storage of OPs. As most of the plant personnel had been evacuated because of natural disasters, only one person was left, and therefore, there were no casualties. However, the entire plant was destroyed [33]. The thermal hazards of OPs have led to many studies [9, 26, 31, 34, 35]. The study also compiled related accidents caused by OPs in the past which is listed in Table 1. However, in previous literature reports, there are

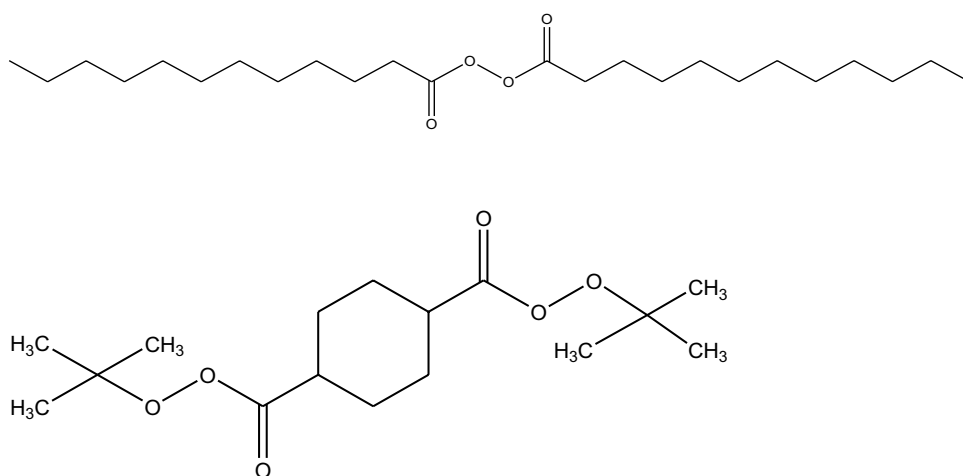**Fig. 2** Basic chemical structures of LPO (top) and HTP-65W (bottom)

Table 1 Selected incidents of fire or explosion caused by organic peroxides

Date	Chemical	Location	Injuries	Fatalities	Hazard	Cause
1990.05.26	BPO	Japan	17	9	Explosion	Thermal decomposition
1996.10.07	MEKPO	Taiwan	47	10	Explosion (tank)	Fire
2000.08.24	MEKPO	Korea	11	3	Explosion (storage)	Unknown
2003.01.02	BPO	USA	1	0	Explosion (dryer)	Thermal decomposition
2003.09.26	CHP/DCPO	Taiwan	2	0	Explosion	
2008.01.16	DCPO	Taiwan	0	0	Explosion (reactor)	Thermal decomposition
2009.06.22	TBHP	Taiwan	0	0	Explosion (reactor)	Thermal decomposition
2010.01.08	CHP	Taiwan	0	0	Explosion (reactor)	Caught fire
2011.07.26	H_2O_2	Taiwan	0	0	Fire	Pipeline gas leak
2014.07.31	Propylene	Taiwan	310	32	Explosion and fire	Pipeline gas leak

Remarks: [a]methyl ethyl ketone peroxide; [b]hydrogen peroxide; [c]tert-butyl hydroperoxide

insufficient thermokinetic analysis results, especially those regarding BPO, LPO, and HTP-65W, along with few related thermal hazard evaluations.

The main objective of the study

Thermokinetic characteristics are essential to the evaluations in this study assessing the magnitude of the thermal hazard of three common OPs, BPO, LPO, and HTP-65W, in industrial processes via two calorimetric techniques and an analytical approach. Differential scanning calorimetry (DSC) combined with a mathematical model has been used for preliminary kinetic analysis of the three OPs [10, 36, 37]. The DSC test at several heating rates (β) and the introduced thermokinetic estimate model [36, 37] brought the thermal hazard assessment and operation closer to real process conditions. The abovementioned kinetic parameters of the three OPs can be discriminated and evaluated based on thermal hazards [38, 39]. These kinetic parameters can be used as the basis for simulating the thermal hazard assessment model of materials under actual conditions [40, 41]. The main principle was to estimate the heat exchange conditions for the materials, container, and surrounding environment to simulate the heat release patterns of the materials in this situation [10, 20, 42, 43], and an evaluation model based on the thermal stability of the reaction was established.

Experimental

Samples

Samples of 75% BPO, 98% LPO, and HTP-65W were purchased from ACE Chemical Corp., Shanghai, China. These samples should be refrigerated in a low-temperature drier to prevent the self-reactive process caused by a temperature increase.

Differential scanning calorimetry

The sample, 5.0 mg of BPO or LPO or 2.5 mg of HTP-65W, was placed in a gold crucible and analyzed using the dynamic scanning technique with a Mettler DSC821^e system [44]. STAR^e software was used to analyze the data curves based on thermal decomposition properties, such as the apparent exothermic onset temperature (T_0), peak temperature at which maximum heat release occurred in reaction (T_p), reaction order (n), heat of decomposition (ΔH_d), pre-exponential factor (A), and apparent activation energy (E_a) [10, 45, 46]. We selected 0.5, 1.0, 2.0, and 4.0 °C min^{-1} as the heating rates [10, 45, 46]. The experimental parameters set the temperature in the range of 30.0–300.0 °C degrees.

The mechanism of the decomposition of BPO, LPO, and HTP-65W

To simulate the thermal hazards of samples, it is necessary to evaluate the reaction kinetic mode and parameters [10, 47]. Reaction kinetics change depending on the reaction type, such as nth order, autocatalytic, or multistage reactions [9, 43]. Different types of reactions can be described by various kinds of kinetic models [10, 34]. In general, information concerning processes (particularly those concerning mixed multistage reactions) is not readily available. System state variables are based on assumptions that can be replaced by the degree of conversion (α) of the reaction [36, 48, 49]. The kinetic model can be simplified to contain the main characteristics of the reaction without the need for the detailed reaction mechanism [10, 36, 37, 50].

In contrast to the product of an nth-order reaction, the product of an autocatalytic reaction acts as a catalyst that accelerates the overall reaction [51]. When the reaction is initially conducted, it is mainly characterized by a slower reaction rate than that of the nth-order reaction until enough catalytic products are produced to accelerate the reaction and the reactant is consumed [52]. Under certain conditions, autocatalytic reactions need to be designed with special consideration for the possibility of thermal runaway [53].

The kinetic complexity of the material in single and complex multistage reactions depends on its internal reaction form, which may be involved in a variety of mutual non-interfering, simultaneous and successive reaction stages acquired from the Arrhenius equation, which expresses reaction characteristics with the reaction functions f(a) as shown in Eqs. (1)–(3) [8, 54].

For a single-stage reaction, the reaction process can be characterized as X→Y:

$$\frac{\mathrm{d}\alpha}{\mathrm{d}t} = f(\alpha)k_0 e^{-\frac{E_a}{RT}} \tag{1}$$

$$f(\alpha) = (1-\alpha)^n \quad n\text{th order model} \tag{2}$$

$$f(\alpha) = (1-\alpha)^{n_1}(\alpha^{n_2} + z) \quad \text{autocatalytic model} \tag{3}$$

where E_a is the activation energy; R is the gas constant; T is the temperature of the sample; α is the degree of conversion of the reactant; k_0 is the pre-exponential factor; n, n_1, and n_2 are the reaction orders; and z is the autocatalytic constant.

For reactions with a continuous reaction phase, X→Y→Z:

$$\frac{\mathrm{d}\alpha}{\mathrm{d}t} = (1-\alpha)^{n_1} k_{01} e^{-\frac{E_{a1}}{RT}} \tag{4}$$

$$\frac{\mathrm{d}\gamma}{\mathrm{d}t} = (1-\alpha)^{n_2} k_{02} e^{-\frac{E_{a2}}{RT}} \tag{5}$$

where γ is the reaction progress of the second stage; E_{a1} and E_{a2} are the activation energies of stages one and two, respectively; and k_{01} and k_{02} are pre-exponential factors.

Multiple reactions occurred simultaneously and independently of each other. For an internal reaction, such as an autocatalytic stage, $X + Y \rightarrow 2Y$:

$$\frac{d\alpha}{dt} = r_1(\alpha) + r_2(\alpha) \tag{6}$$

$$r_1(\alpha) = k_{01}e^{-\frac{E_1}{RT}}(1-\alpha)^{n_{11}} \tag{7}$$

$$r_2(\alpha) = k_{02}e^{-\frac{E_2}{RT}}\alpha^{n_{21}}(1-\alpha)^{n_{22}} \tag{8}$$

where r_1 and r_2 are reaction rates of different stages and n is the reaction order. The reaction form of the autocatalytic reaction is the main characteristic of this method.

The reaction product can further catalyze and increase the reaction rate, and Eq. (6) can be rewritten for an autocatalytic reaction mode that assumes that $n_{11} = n_{22} = n_1$ and $n_{21} = n_2$:

$$\begin{aligned} \frac{d\alpha}{dt} &= k_{01}e^{-\frac{E_{a1}}{RT}}(1-\alpha)^{n_{11}} + k_{02}e^{-\frac{E_{a2}}{RT}}\alpha^{n_{21}}(1-\alpha)^{n_{22}} \\ &= k_{02}(1-\alpha)^{n_1}(\alpha^{n_2} + z(T))\exp\left(-\frac{E_{a2}}{RT}\right) \end{aligned} \tag{9}$$

$$z(T) = \frac{k_{01}}{k_{02}}\exp\left(-\frac{E_{a1}-E_{a2}}{RT}\right) = z_0\exp\left(-\frac{E_z}{RT}\right) \tag{10}$$

where z_0 is the ratio of the pre-exponential factors k_{01}/k_{02} and $E_z = E_1 - E_2$.

The model is established by representing the property of autocatalytic reactions for fitting thermal data [55].

Simulating thermal behavior under process conditions

After assessing the reaction kinetics of the material, the pattern of heat transfer between the substance and its surroundings, such as the container, can be estimated. In the large-scale case, the heat generated by the sample may not immediately exchange with its surroundings. As a result, heat exchange between the sample and the environment can be assumed to be a possible pathway of heat accumulation in the system, which increases the system temperature in an unrestrained way and causes a runaway reaction. The variety of reaction modes makes the nonlinear fitting method adaptable. When a material stored in a container is accompanied by heat exchange with the surrounding environment, the following heat conduction equations can be used [10, 36, 37]:

$$\rho C_p \frac{\partial T}{\partial t} = \text{div}(\lambda(\text{grad}(T))) + W \tag{11}$$

where ρ is the density; C_p is the specific heat capacity; λ is the thermal conductivity coefficient; T is the temperature; and W is the generated heat.

Assuming that the initial temperature in the container is evenly distributed,

$$T|_{t=0} = T_i \tag{12}$$

The boundary conditions to be considered are given in Eqs. (13) to (15).

1st kind: $\quad T_w = T_e \tag{13}$

2nd kind: $\quad -\lambda\frac{\partial T}{\partial X}|_w = q_e \tag{14}$

3rd kind: $\quad \lambda\frac{\partial T}{\partial X}|_w = U(T_w - T_e) \tag{15}$

where x is the unit outer normal with a boundary; w and e are the surface of the reaction and environment, respectively; and U is the heat transfer coefficient.

Simulating thermokinetics by the maximum rate (*TMR*) under the pseudoadiabatic condition in different temperature ranges

Decomposition reactions are not conducive to the storage of materials. Materials in large-scale packaging or storage are more susceptible to thermal hazards due to heat dissipation than those in decentralized packaging. The accumulation of heat in a short period of time is not obvious, but it may be accompanied by a specific risk of long residence time and heat build-up due to the hindered heat transfer from the bulk material to the surrounding environment. High-temperature environments increase the reaction rate. Heat accumulation-induced reactions will continue even at lower temperatures. This behavior suggests that under different process conditions, such as adiabatic and isothermal conditions, the decomposition reaction will reach the maximum rate in a period of time, called the TMR_{ad} and TMR_{iso} for pseudoadiabatic and isothermal conditions, respectively [46, 56]. An increase in the reaction rate indicates that the reaction is resistant to control by external factors, suggesting that the TMR_{ad} and TMR_{iso} at the highest storage temperature are the most important features for determining the reaction time required for process operation or emergency response.

TMR_{ad} and TMR_{iso} can be obtained by adiabatic or isothermal calorimetry techniques, such as the vent sizing package 2 and the thermal activity monitor, respectively. However, the instrument itself and the supplies are valuable, and

Fig. 3 Thermal curves of heat flow *vs* temperature for BPO, HTP-65W, and LPO acquired by DSC at heating rates of 0.5, 1.0, 2.0, and 4.0 °C min^{-1}
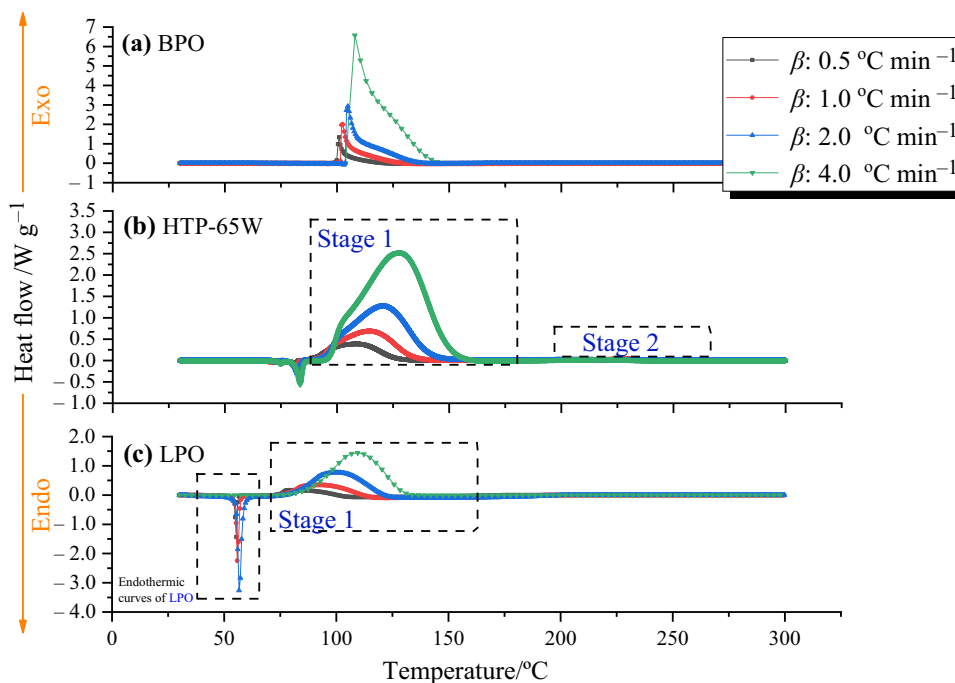

Table 2 Non-isothermal data from DSC tests of BPO, HTP-65W, and LPO at 0.5, 1.0, 2.0, and 4.0 °C min^{-1}

OPs		Heating rate	Melting		Exothermic	
Substance	Mass/mg	β/°C min^{-1}	T_m/°C	ΔH_d/J g^{-1}	T_0/°C	ΔH_d/J g^{-1}
BPO 75 mass%	5 ± 0.2	0.5	–	–	91	1087
		1.0	–	–	95	1031
		2.0	–	–	102	1247
		4.0	–	–	106	1065
HTP-65W 98 mass%	2.5 ± 0.2	0.5	68	−52	83	1142
		1.0	65	−53	86	1115
		2.0	67	−51	92	1136
		4.0	68	−54	95	1223
LPO 98 mass%	5 ± 0.2	0.5	45	−74	65	555
		1.0	46	−77	72	764
		2.0	47	−72	72	765
		4.0	47	−71	73	786

the experiment steps are time-consuming [13, 57]. Relatively fast and basic calorimetry, such as DSC, can be efficient for scale-up.

Regarding chemical processes, TMR_{ad} have been established based on dynamic DSC measurements for the early stages. Thermal hazards are associated with the energy generated by decomposition, such as heat release or excessive gaseous products damaging external structures. From [10], the decomposition mechanism combined with mathematical models leads to the specific thermokinetics for the Thermal Safety software [58] and the Kinetics software developed by the Netzsch Group [27, 43]. The thermal hazard model is simulated by the inherent kinetics model with DSC data. The consistent adiabatic temperature rise can also be estimated.

Thermal stability determined by time to conversion limit, self-accelerating decomposition temperature, control temperature, and emergency temperature

If the material is stored at a higher ambient temperature, the reaction rate will rise in a short time and cause thermal runaway. However, long-term storage may still cause potential safety hazards. The self-reaction characteristics of the substance itself are combined with a large number of material environments, and the heat accumulation of the material will also gradually increase the reaction rate, which will eventually cause uncontrolled reactions. Therefore, by evaluating the amount of material consumed by the reaction at a certain level in a certain period of time (time to reach the conversion
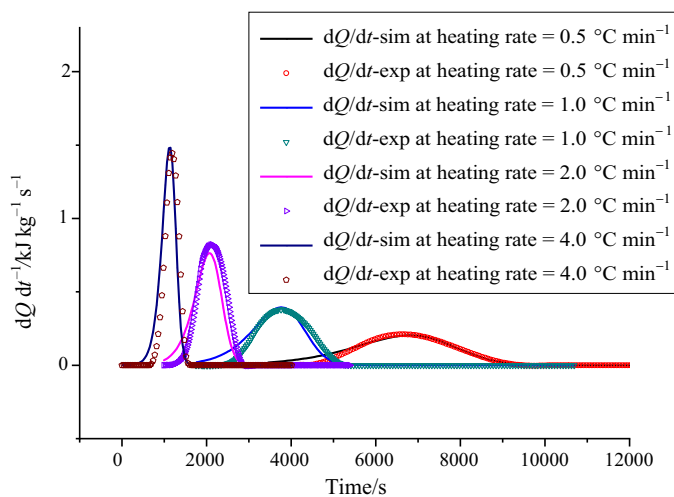
Fig. 4 Comparisons of BPO, HTP-65, and LPO heat production rate versus time curves at heating rates of 0.5, 1.0, 2.0, and 4.0 °C min^{-1} obtained by experiments and simulations
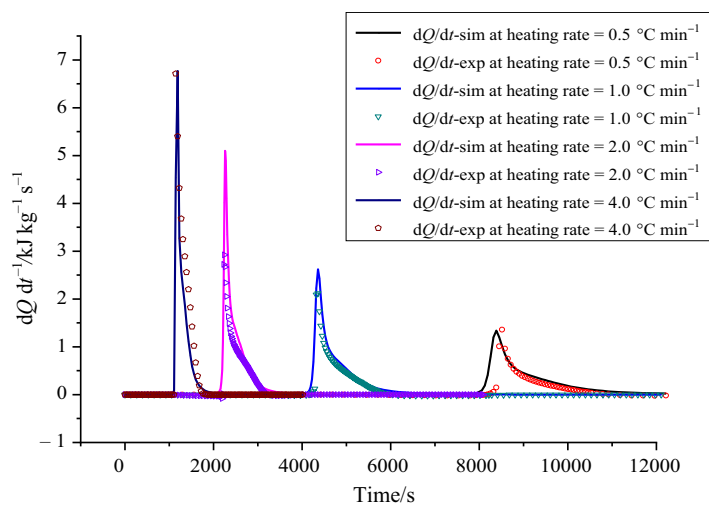
(a) BPO
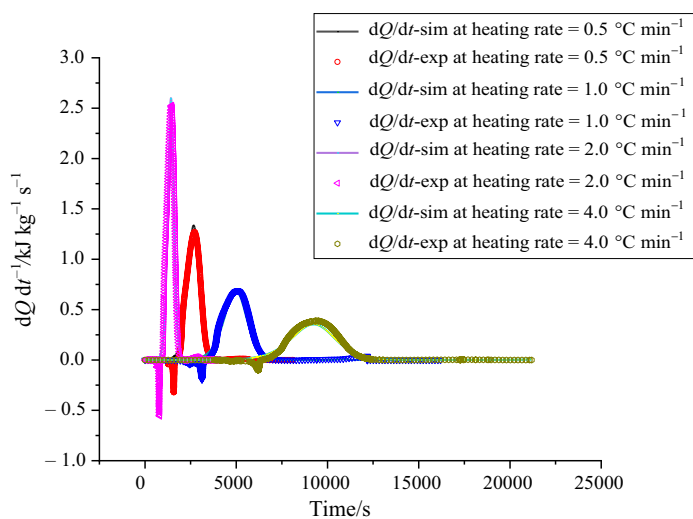
(b) HTP-65W

(c) LPO

limit, *TCL*), the danger of the reaction that may be caused by the current ambient temperature can be determined.

The degree of hazard of self-accelerating decomposition reactions of substances mainly depends on ambient temperature and the form of packaging. According to U.S. Department of Transportation Pipeline and Hazardous Materials Safety Administration with Title 49 of the Code of Federal Regulations, Subchapter C, "Hazardous Materials Regulations" Parts 171.22, self-accelerating decomposition temperature (*SADT*), control temperature (*CT*), and emergency temperature (*ET*) are utilized for evaluating the thermal safety conditions. Based on the definition of *SADT* [22, 59–63], we combined the kinetic models obtained in "The mechanism of the decomposition of BPO, LPO, and HTP-65W" and "Simulating thermal behavior under process conditions" sections, and the exothermic models of OPs in different environmental systems are simulated with Eq. (16) for describing *SADT*:

$$\frac{\mathrm{d}T}{\mathrm{d}t} = \frac{\lambda}{\rho C_p}\left(\frac{\partial^2 T}{\partial x^2} + \frac{g}{r}\frac{\partial T}{\partial x}\right) + \frac{-\Delta H_d}{C_p}\frac{\mathrm{d}\alpha}{\mathrm{d}t} \qquad (16)$$

where C_p is the sample heat capacity, λ is the thermal conductivity, ρ is the density of OPs, x is the package radius, and g is a geometry factor that varies by the type of packaging. Furthermore, ΔH_d and $\mathrm{d}\alpha/\mathrm{d}t$ were determined from DSC and "Scale-up and critical runaway parameter analysis by kinetics-based modeling" section [37, 48, 60], respectively. The values of *CT* and *ET* depend on *SADT* [48]. When the ambient temperature exceeds the value of *CT*, the packaging of the material may not be suitable for storage and transportation. Temperatures above the *ET* require urgent measures to address imminent thermal hazards.

Results and discussion

DSC results for the kinetic approach

The thermal curves of three OPs, BPO, HTP-65W, and LPO, as shown in Fig. 3, displayed thermal behavior typical of a solid sample that had an endothermic peak arising from the phase change during the decomposition processes listed in Table 2. Using LPO data as an example, the experimental curve acquired at 4 °C min^{-1} illustrated the existence of a melting phenomenon that appeared as endothermic peak at 50 °C; the endothermic value was 71 J^{-1} g. In addition, the exothermic curve indicated that the onset temperature was 65 °C, and the apex on the thermal curve demonstrated a maximum heat release of 1.5 mW g^{-1}, which occurred at 120 °C. Through analysis of the exothermic curve, the heat released by decomposition was 786 J g^{-1}, revealing the thermal hazard characteristics of LPO.

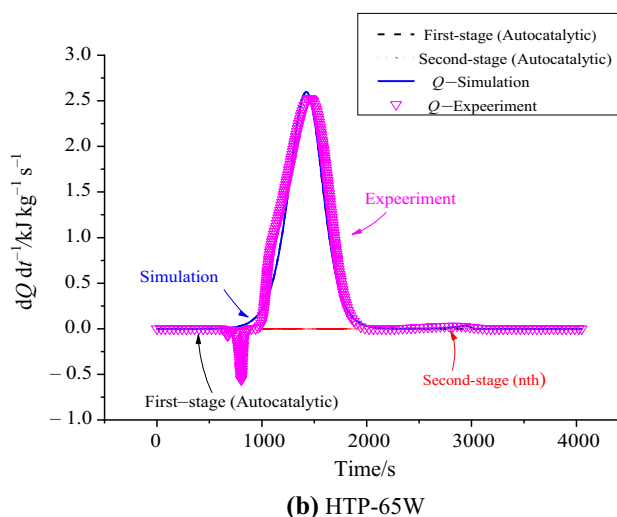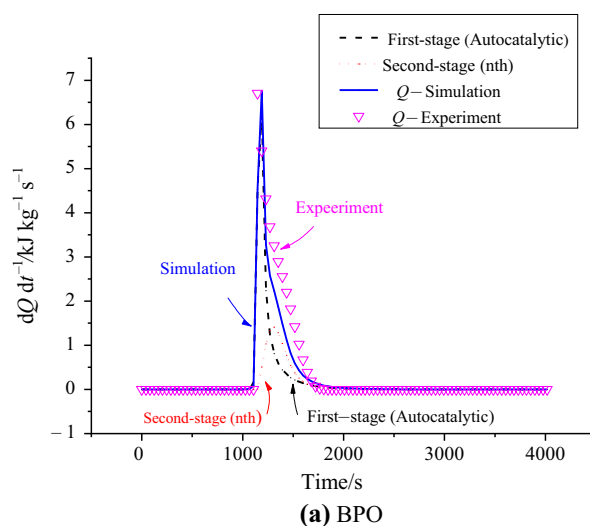
(a) BPO

(b) HTP-65W

Fig. 5 Simulation results of two stages (BPO) (HTP-65W) reaction form into heat production rate with heating rates of BPO and HTP-65W with 4.0 and 2.0 °C min^{-1}, respectively

LPO had a lower T_0 than BPO and HTP-65W. This result, in conjunction with information about the actual operating conditions of OPs, which are often used at 70–80 °C, leads to the conclusion that LPO is more likely to cause reactive hazards than BPO or HTP-65W.

The identification of possible hazards and risks as early as possible is essential for the storage and transportation of raw materials and for production lines. DSC measurements are useful in this regard because basic thermokinetic parameters can be rapidly measured with fewer samples, cooperating nonlinear fitting with flexible space of application to plurality reaction modes and simulated parameters that require large-scale experiments.

Table 3 Kinetics parameter evaluation results of BPO, HTP-65W, and LPO at 0.5, 1.0, 2.0, and 4.0 °C min^{-1}

Sub.	Type	Parameter Units	$\ln(k_0)$ $\ln(1/s)$	E_a kJ mol^{-1}	n_1	n_2^*	z^*	ΔH_d J g^{-1}
					Dimensionless			
BPO	Auto + nth	1st stage	31	203	2.54	0.42	0.0006	30
		2nd stage	42	148	1.9	–	–	1200
HTP-65W	Auto	1st stage	37	139	1.57	0.12	1.37×10^{-6}	1113
		2nd stage	44	203	0.2	0.2	0.0003	1200
LPO	nth	1st stage	30	115	0.9	–	–	744

*Only for autocatalysis reaction

Scale-up and critical runaway parameter analysis by kinetics-based modeling

Based on actual experimental data, reaction kinetic simulations were applied to perform nonlinear fitting. The result of the fitting of heat production rates is shown in Fig. 4. According to Figs. 4a, b and 5a, b, BPO and HTP-65W have multistage reactions that are different from those of LPO, which proceeds through single nth-order reactions, as shown in Fig. 4c. The decomposition of BPO involves simultaneous autocatalytic and nth reactions; in contrast, the reaction of HTP-65W comprised two-stage autocatalysis reactions. The reactions of both BPO and HTP-65W are composed of endothermic and exothermic processes. Kinetic models can be used for determining process operation, such as the temperature required for the procedure, reaction rate, and activation energy, which can further be derived as simulations of the reaction mode. The required evaluation parameters are shown in Table 3.

The simulated conditions in this study involved placing the OPs into 10 (HTP-65W) and 20 kg (BPO and LPO) boxes and 20 (HTP-65W) and 50 (BPO and LPO) kg drums of UN packaging as boundary conditions, which are listed in Tables 4 and 5. Then, we evaluated the heat transfer situation between the package and surroundings to assess what circumstances will lead to runaway reactions and to determine thermal hazard parameters. The material is separated from the package by a plastic bag. Incomplete contact may cause the heat exchange simulation to be different from the actual conditions.

For the external environment, three kinds of situation conditions were set: room temperature (25 °C), heat accumulation causing a higher temperature of 55 °C due to improper heat dissipation, and an external heat source increasing the temperature to T_0.

Table 4 Physical parameters of packages for BPO, HTP-65W, and LPO

Package	material	Size/cm	Shell thickness/mm	Filling height/cm	Density/ g cm^{-3}	Specific heat capacity/J g^{-1} K^{-1}	Thermal conductivity coefficient/W m^{-1} K^{-1}
20 kg Box	BPO and LPO	$L \times W \times H$ $29 \times 39 \times 46$	5.0	35	0.75	1.7	0.3
50 kg Drum		$R \times H$ 19×42	5.0	35	0.75	1.7	0.3
10 kg Box	HTP-65W	$L \times W \times H$ $15 \times 20 \times 40$	5.0	35	0.75	1.7	0.3
20 kg Drum		$R \times H$ 10×21	5.0	35	0.75	1.7	0.3

Table 5 Boundary conditions of packages for BPO, HTP-65W, and LPO

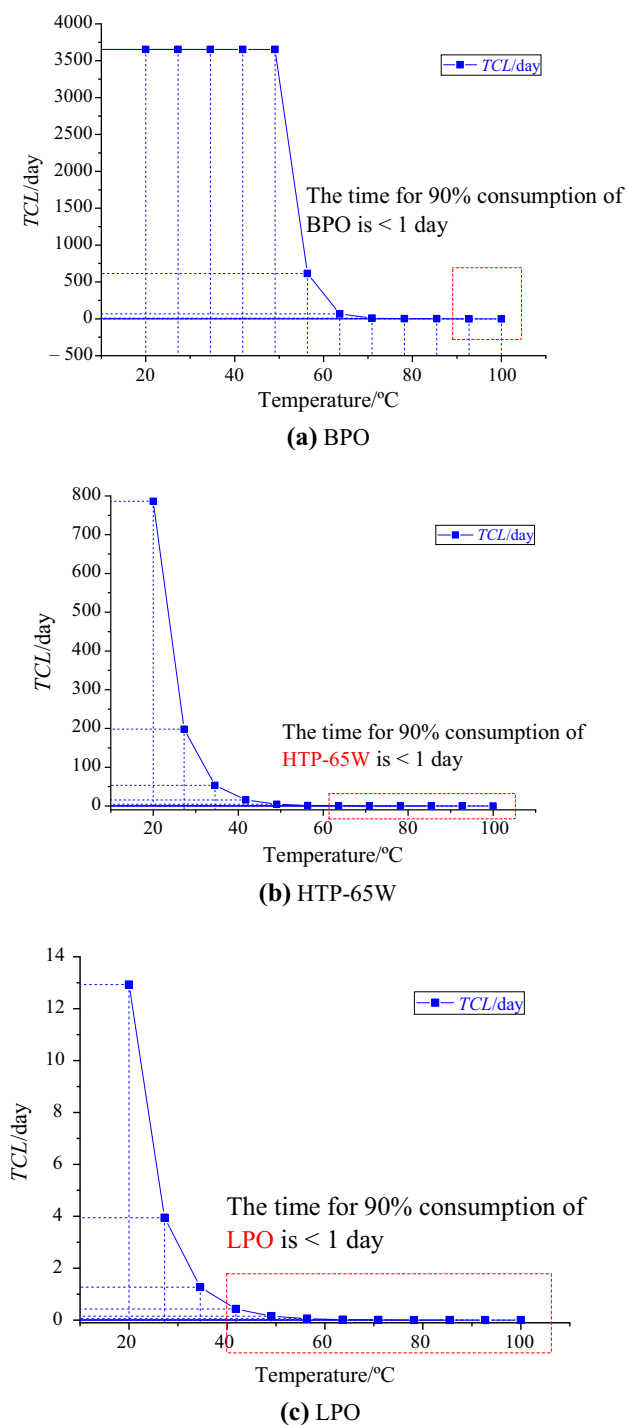| Material	Mass/kg	Environment temperature/°C			Density/g cm^{-3}	Specific heat capacity/J g^{-1} K^{-1}	Thermal conductivity coefficient/W m^{-1} K^{-1}
BPO	20	25	55	73	0.96	1.74	0.1
	50						
HTP-65W	10	25	55	85	0.95	2.00	0.1
	20						
LPO	20	25	55	73	0.96	1.55	0.1
	50						

(a) BPO

(b) HTP-65W

(c) LPO

Fig. 6 Simulation results for the *TCL* of BPO, HTP-65W, and LPO at different ambient temperatures and a heating rate of 4.0 °C min^{-1}

The storage, transportation, and reaction safety parameters of BPO, HTP-65W, and LPO are shown in Fig. 6 and Table 6, which contain the determined values of the *SADT*, *TCL*, *CT*, and *ET*. In contrast to BPO and HTP-65W, LPO is immediately consumed (> 90%) in one day when the lower temperature limit (< 40 °C). The values of *SADT*,

Table 6 Results of thermal explosion simulations of BPO, HTP-65W, and LPO

Material	Shape	SADT/°C	CT/°C	ET/°C
BPO	20 kg Box	70	60	65
	50 kg Drum	69	59	64
HTP-65W	10 kg Box	44	34	39
	20 kg Drum	27	17	22
LPO	20 kg Box	24	9	14
	50 kg Drum	24	9	14

CT, and *ET* being less than 40 °C indicate that LPO has potential thermal hazards in an environment above this temperature.

The type of package will appreciably affect the thermal stability of HTP-65W. Regarding thermal safety for storage and transportation, *SADT*, *CT*, and *ET* are significant quantitative criteria for describing whether a material should have its temperature controlled by cooling systems, such as ventilation facilities, during storage and transportation. Moreover, for the larger packaged HTP-65W, heat accumulation may accelerate the reaction rate by an autocatalytic reaction. It is necessary to guarantee thermal safety during the storage and transportation of HTP-65W. Although the state of the package has no obvious effect on LPO under transportation and storage conditions, it still needs to be stored at low temperatures.

The *TMR*$_{ad}$ results are shown in Fig. 7. The reaction rate was significantly correlated with thermal safety. A fast reaction rate can decrease the process time. However, if the temperature and pressure increases caused by the heat and gas products released cannot be appropriately controlled, the runaway reaction occurred, especially when the process reached the maximum reaction rate. Therefore, *TMR*$_{ad}$ is an essential factor in assessing process hazards. Compared to HTP-65W and BPO, LPO had a shorter *TMR*$_{ad}$ when temperatures ≤ 50 °C. HTP-65W had a relatively longer *TMR*$_{ad}$, even if the temperature was > 63 °C. The longer *TMR*$_{ad}$ also meant that there is ample time to regulate the process into normalization. For storage and transportation, the degree of hazard can be expressed from the highest to the lowest as LPO > HTP-65W > BPO. *TMR*$_{ad}$ defines the conditions under which a material or a process becomes thermally unstable or a thermal runaway.

Kinetic descriptions of chemical reactions can be used to estimate their thermal behavior profiles at any temperature. This procedure can be used for risk analysis of chemical compounds or processes to ensure safe working conditions and minimize possible risks to production and actual operations. The hazard characteristics are consistent with the runaway conditions of OPs under different temperatures, as shown in Figs. 8 and 9. When the temperature exceeds
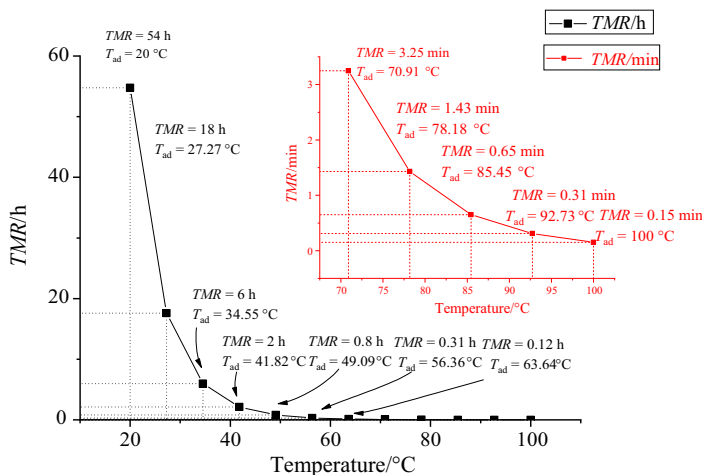
Fig. 7 Simulation results for the TMR_{ad} of BPO, HTP-65W, and LPO at different ambient temperatures and a heating rate of 4.0 °C min^{-1}
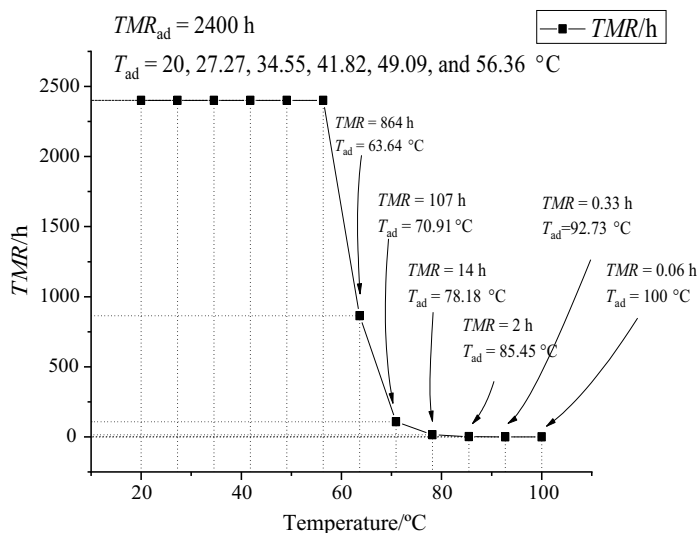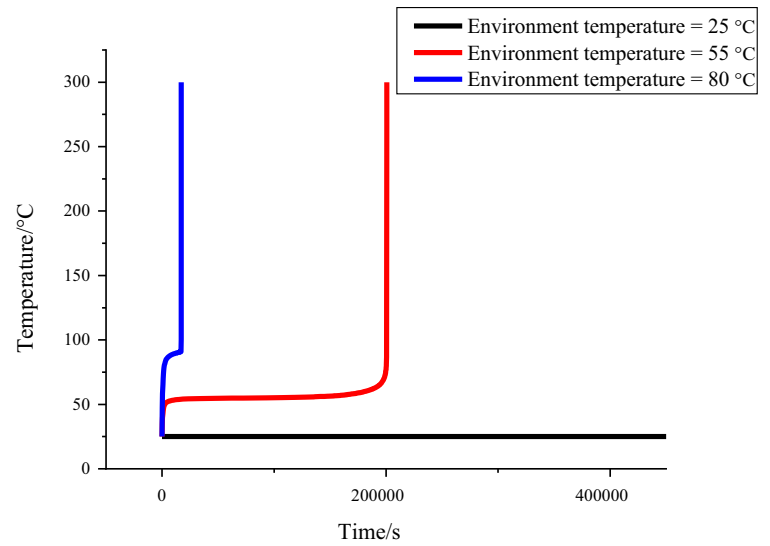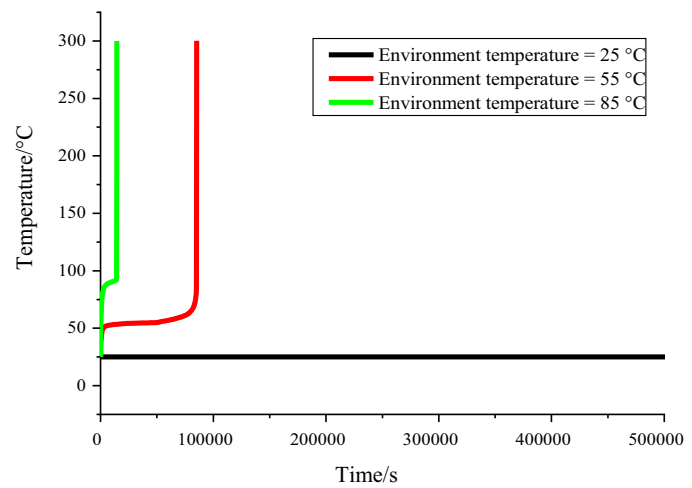

(a) BPO
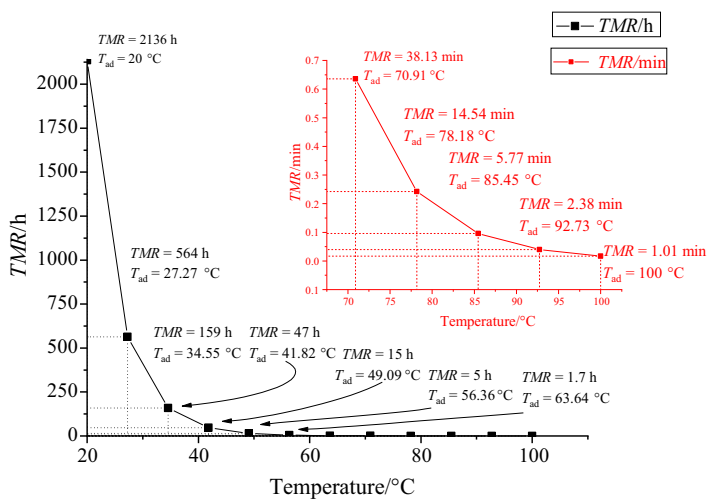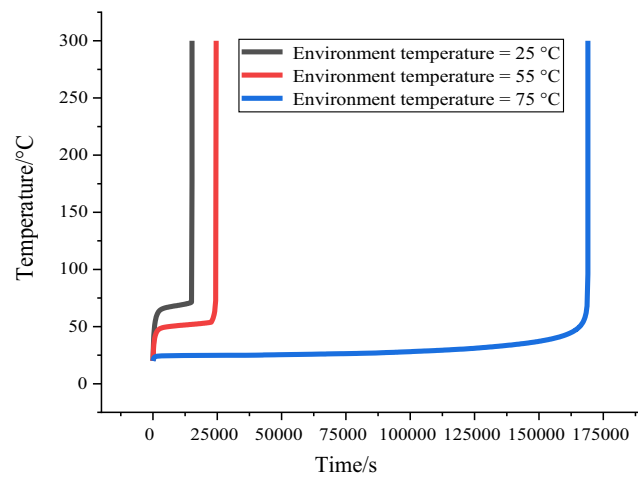

(b) HTP-65W

(c) LPO

Fig. 8 Simulation results of runaway reactions of BPO, HTP-65W, and LPO with box packaging at different ambient temperatures
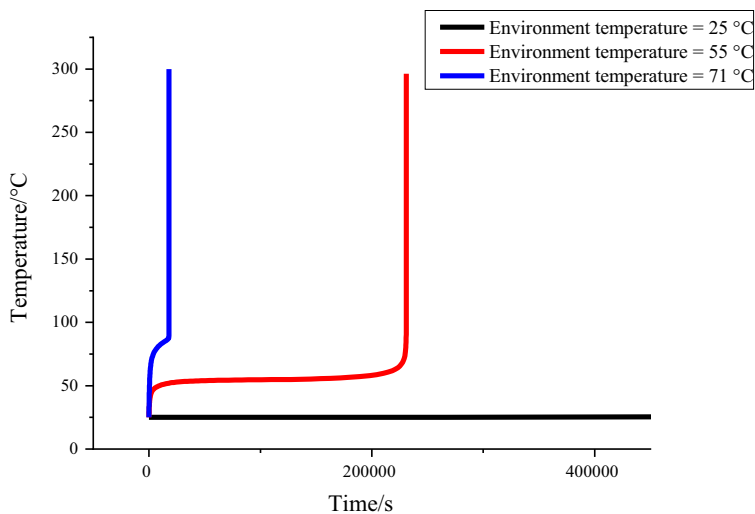

(a) BPO
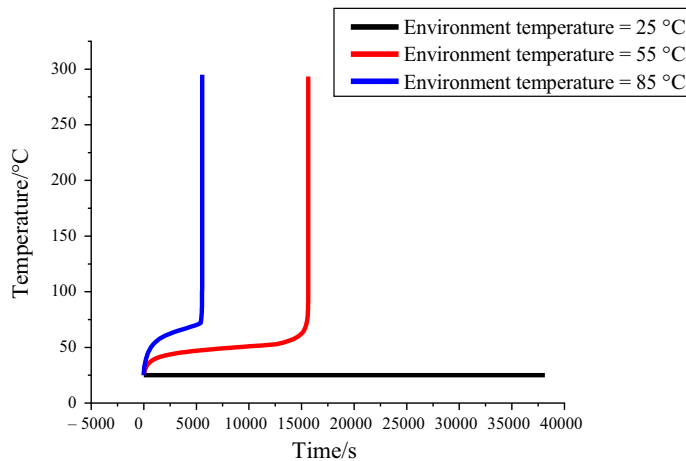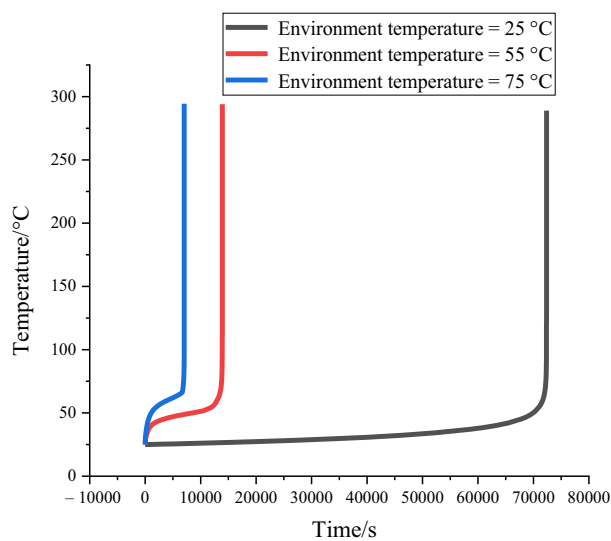

(b) HTP-65W

(c) LPO

Fig. 9 Simulation results of runaway reactions of BPO, HTP-65W, and LPO with drum packaging at different ambient temperatures

(a) BPO

(b) HTP-65W

(c) LPO

a certain level, the decomposition reaction will cause the occurrence of a runaway reaction. However, in contrast to LPO, BPO and HTP-65W did not produce runaway reactions at room temperature (25 °C), which must be due to heat removal efficiency. From the simulation results, the form of packaging has a significant impact on HTP-65 and LPO's thermal safety under runaway conditions. The main difference is the reduction in time required to reach thermal runaway. In an actual process, the OPs should be refrigerated, and the protection against heat accumulation should be constantly enhanced. The processes in the chemical industry with an active decomposition reaction are usually implemented in a high-temperature environment. If the monitoring of reaction progress is inadequate, even a slight temperature change may result in thermal runaway due to the extremely rapid reaction speed.

Conclusions

The data obtained through a series of tests on the thermal runaway reactions of BPO, HTP-65W, and LPO were initially studied using a non-isothermal DSC experiment. The kinetic mode is determined to predict heat transfer on a large scale based on the reaction parameters of the three OPs. This approach can be used to reduce the number of cumbersome and expensive actual-scale experiments. Considering the thermal behavior of a reaction in a simulation can contribute to avoiding thermal hazards in real situations.

The characteristic parameters, such as $SADT$, CT, TMR_{ad}, and ET, for the thermal decomposition of LPO obtained by mathematical methods showed that if the temperature reached 50 °C, the thermal stability decreased; therefore, for storage and transportation, much attention should be paid to cooling measurements.

Unlike BPO and HTP-65W, LPO still induced runaway reactions at temperatures lower than 25 °C. Thus, LPO should be refrigerated during storage and transportation. To balance and promote safety measures for the use of BPO, HTP-65W, and LPO during processes, accident prevention for BPO, HTP-65W, and LPO during storage and transportation should be emphasized, as these are the significant and key issues for the future.

References

1. Murray R, Snowberg DR, Berry DS, Beach R, Rooney, SA, Swan D, Manufacturing a 9-meter thermoplastic composite wind turbine blade. National Renewable Energy Lab. (NREL), Golden, CO (United States). 2017.
2. Oliveira MCC, Diniz Cardoso ASA, Viana MM, Lins VDFC. The causes and effects of degradation of encapsulant ethylene vinyl acetate copolymer (EVA) in crystalline silicon photovoltaic modules: a review. Renew Sustain Energy Rev. 2018;81:2299–317.
3. Hejna A, Klein M, Saeb MR, Formela K. Towards understanding the role of peroxide initiators on compatibilization efficiency of thermoplastic elastomers highly filled with reclaimed GTR. Polym Test. 2019;73:143–51.
4. Przybysz M, Marć M, Klein M, Saeb MR, Formela K. Structural, mechanical and thermal behavior assessments of PCL/PHB blends reactively compatibilized with organic peroxides. Polym Test. 2018;67:513–21.
5. AkzoNobel. Nouryon completes further peroxides expansions; reports growth in first annual results. Addit Polym. 2019;2019:6–7.
6. AkzoNobel. Nouryon to double capacity for solvent-based organic peroxides in Mexico. Addit Polym. 2019;2019:9.
7. Chervin S, Bodman GT. Method for estimating decomposition characteristics of energetic chemicals. Process Saf Prog. 2003;22:241–3.
8. Levin M, Gonzales N, Zimmerman L, Yang J. Kinetics of acid-catalyzed cleavage of cumene hydroperoxide. J Hazard Mater. 2006;130:88–106.
9. Talouba IB, Balland L, Mouhab N, Abdelghani-Idrissi M. Kinetic parameter estimation for decomposition of organic peroxides by means of DSC measurements. J Loss Prev Process Ind. 2011;24:391–6.
10. Wang SY, Kossoy AA, Yao YD, Chen LP, Chen WH. Kinetics-based simulation approach to evaluate thermal hazards of benzaldehyde oxime by DSC tests. Thermochim Acta. 2017;655:319–25.
11. Wilberforce J. The use of the accelerating rate calorimeter to determine the SADT of organic peroxides. Milton Keynes: Columbia Scientific Industries; 1981.
12. Dannley R. Organic peroxides: their formation and reactions (Hawkins, E. G. E.). J Chem Educ. 1963;40:A62.
13. Wang Q, Rogers WJ, Mannan MS. Thermal risk assessment and rankings for reaction hazards in process safety. J Therm Anal Calorim. 2009;98:225–33.
14. SpecialChem, Organic peroxides market to reach $1069.1 M by 2022, Focus Surfactants, 2017;4.
15. Dizay H, Lau D, Nottage WM. Benzoyl peroxide and clindamycin topical skin preparation decreases Propionibacterium acnes deep colonization in shoulder arthroscopy. J Shoulder Elbow Surg. 2017;26:162.
16. Sparavigna A, Tenconi B, De Ponti I, La Penna L. An innovative approach to the topical treatment of acne. Clin Cosmet Investig Dermatol. 2015;8:179–85.
17. AkzoNobel. AkzoNobel strengthens global organic peroxides business with Mexican expansion. Addit Polym. 2017;2017:9.
18. AkzoNobel. AkzoNobel expands Mexican organic peroxide capacity, plans further increase in China. Addit Polym. 2017;2017:5–6.
19. United Nations. Recommendations on the transport of dangerous goods: model regulations (Twentieth Revised Edition). New York: United Nations Publications; 2018.
20. Di SI, Marotta R, Andreozzi R, Caprio V. Kinetic and chemical characterization of thermal decomposition of dicumylperoxide in cumene. J Hazard Mater. 2011;187:157–63.
21. Hou HY, Duh YS, Lee WL, Shu CM. Hazard evaluation for redox system of cumene hydroperoxide mixed with inorganic alkaline solutions. J Therm Anal Calorim. 2009;95:541–5.
22. Steensma M, Schuurman P, Malow M, Krause U, Wehrstedt KD. Evaluation of the validity of the UN SADT H.4 test for solid

organic peroxides and self-reactive substances. J Hazard Mater. 2005;117:89–102.

23. Wang YW, Duh YS, Shu CM. Evaluationof adiabatic runaway reaction and vent sizing for emergency relief from DSC. J Therm Anal Calorim. 2006;85:225–34.

24. Lin CP, Tseng JM, Chang YM, Liu SH, Cheng YC, Shu CM. Modeling liquid thermal explosion reactor containing tert-butyl peroxybenzoate. J Therm Anal Calorim. 2010;102:587–95.

25. Zhu Y, Chen Y, Zhang L, Li W, Huang B, Wu J. Numerical investigation and dimensional analysis of reaction runaway evaluation for thermal polymerization. Chem Eng Res Des. 2015;104:32–41.

26. Huang YH. I YP, Chen NC, Wu SH, Horng JJ, Wu YT, Wen IJ, Thermal runaway reaction evaluation of benzoyl peroxide using calorimetric approaches. J Therm Anal Calorim. 2013;113:595–8.

27. Opfermann J, Hädrich W. Prediction of the thermal response of hazardous materials during storage using an improved technique. Thermochim Acta. 1995;263:29–50.

28. Wu KW, Hou HY, Shu CM. Thermalphenomena studies for dicumyl peroxide at various concentrations DSC. J Therm Anal Calorim. 2006;83:41–4.

29. Zhang Y, Ni L, Jiang J, Jiang J, Zhang W, Jiang J, Zhang M. Thermal hazard analyses for the synthesis of benzoyl peroxide. J Loss Prev Process Ind. 2016;43:35–41.

30. Chiang CL, Liu SH, Lin YC, Shu CM. Thermal release hazard for the decomposition of cumene hydroperoxide in the presence of incompatibles using differential scanning calorimetry, thermal activity monitor III, and thermal imaging camera. J Therm Anal Calorim. 2017;127:1061–9.

31. Wu SH, Shyu ML, Yet-Pole I, Chi JH, Shu CM. Evaluation of runaway reaction for dicumyl peroxide in a batch reactor by DSC and VSP2. J Loss Prev Process Ind. 2009;22:721–7.

32. You ML, Liu MY, Wu SH, Chi JH, Shu CM. Thermal explosion and runaway reaction simulation of lauroyl peroxide by DSC tests. J Therm Anal Calorim. 2009;96:777–82.

33. Arkema, Arkema's Crosby peroxides plant suffers hurricane-related damage. Addit Polym. 2017;7.

34. Chen WC, Shu CM. Prediction of thermal hazard for TBPTMH mixed with BPO through DSC and isoconversional kinetics analysis. J Therm Anal Calorim. 2016;126:1937–45.

35. Zaman F, Beezer AE, Mitchell JC, Clarkson Q, Elliot J, Davis AF, Willson RJ. The stability of benzoyl peroxide by isothermal microcalorimetry. Int J Pharm. 2001;227:133–7.

36. Kossoy AA, Akhmetshin YG. Simulation-based approach to design of inherently safer processes. Process Saf Environ Prot. 2012;90:349–56.

37. Kossoy AA, Belokhvostov VM, Koludarova EY. Thermal decomposition of AIBN: Part D: Verification of simulation method for SADT determination based on AIBN benchmark. Thermochim Acta. 2015;621:36–43.

38. Brown ME, Maciejewski M, Vyazovkin S, Nomen R, Sempere J, Burnham A, Opfermann J, Strey R, Anderson HL, Kemmler A, Keuleers R, Janssens J, Desseyn HO, Li CR, Tang TB, Roduit B, Malek J, Mitsuhashi T. Computational aspects of kinetic analysis: Part A: The ICTAC kinetics project-data, methods and results. Thermochim Acta. 2000;355:125–43.

39. Burnham AK. Computational aspects of kinetic analysis: Part D: The ICTAC kinetics project–multi thermal history model fitting methods and their relation to isoconversional methods. Thermochim Acta. 2000;355:165–70.

40. Dai X, Shi L, An Q, Qian W. Chemical kinetics method for evaluating the thermal stability of Organic Rankine Cycle working fluids. Appl Therm Eng. 2016;100:708–13.

41. Duh YS, Kao CS, Lee WLW. Chemical kinetics on thermal decompositions of dicumyl peroxide studied by calorimetry. J Therm Anal Calorim. 2017;127:1089–98.

42. Liu SH, Lin CP, Shu CM. Thermokinetic parameters and thermal hazard evaluation for three organic peroxides by DSC and TAM III. J Therm Anal Calorim. 2011;106:165–72.

43. Opfermann J. Kinetic analysis using multivariate non-linear regression. I. Basic concepts. J Therm Anal Calorim. 2000;2011(60):641–58.

44. Mettler TA8000, MT, Columbus, Ohio, USA, STARe software with solaris operating system. Operating Instructions, Switzerland. 1998.

45. Liu SH, Hou HY, Shu CM. Thermal hazard evaluation of the autocatalytic reaction of benzoyl peroxide using DSC and TAM III. Thermochim Acta. 2015;605:68–76.

46. Liu SH, Shu CM. Advanced technology of thermal decomposition for AMBN and ABVN by DSC and VSP2. J Therm Anal Calorim. 2015;121:533–40.

47. Martín-Lara M, Blázquez G, Zamora M, Calero M. Kinetic modeling of torrefaction of olive tree pruning. Appl Therm Eng. 2017;113:1410–8.

48. Kossoy AA, Akhmetshin YG. Identification of kinetic models for the assessment of reaction hazards. Process Saf Prog. 2007;26:209–20.

49. Kossoy AA, Sheinman IY. Comparative analysis of the methods for SADT determination. J Hazard Mater. 2007;142:626–38.

50. Kossoy AA, Benin AI, Akhmetshin YG. An advanced approach to reactivity rating. J Hazard Mater. 2005;118:9–17.

51. Andreozzi A, Buonomo B, Manca O. Numerical study of natural convection in vertical channels with adiabatic extensions downstream. Numer Heat Transf Part A. 2005;47:741–62.

52. Neylon MK, Savage PE. Analysis of non-isothermal heterogeneous autocatalytic reactions. Chem Eng Sci. 1996;51:851–8.

53. Parulekar SJ. Modal analysis and optimization of isothermal autocatalytic reactions. Chem Eng Sci. 1998;53:2379–94.

54. Kossoy AA, Hofelich TC. Methodology and software for assessing reactivity ratings of chemical systems. Process Saf Prog. 2003;22:235–40.

55. Beckmann JW, Wilkes JS, McGuire RR. 2,4,6-Trinitrotoluene thermal decomposition: kinetic parameters determined by the isothermal differential scanning calorimetry technique. Thermochim Acta. 1977;19:111–8.

56. Wang TS, Liu SH, Qian XM, You ML, Chou WL, Shu CM. Isothermal hazards evaluation of benzoyl peroxide mixed with benzoic acid via TAM III test. J Therm Anal Calorim. 2013;113:1625–31.

57. Huang CC, Peng JJ, Wu SH, Hou HY, You ML, Shu CM. Effects of cumene hydroperoxide on phenol and acetone manufacturing by DSC and VSP2. J Therm Anal Calorim. 2010;102:579–85.

58. ChemInform Saint-Petersburg (CISP), L., Thermal Safety Software. http://www.cisp.spb.ru, 2019.

59. Li XR, Koseki H. SADT prediction of autocatalytic material using isothermal calorimetry analysis. Thermochim Acta. 2005;431:113–6.

60. Lv J, Chen L, Chen W, Gao H, Peng M. Kinetic analysis and self-accelerating decomposition temperature (SADT) of dicumyl peroxide. Thermochim Acta. 2013;571:60–3.

61. Malow M, Wehrstedt KD. Prediction of the self-accelerating decomposition temperature (SADT) for liquid organic peroxides from differential scanning calorimetry (DSC) measurements. J Hazard Mater. 2005;120:21–4.

62. Gao PF, Liu SH, Zhang B, Cao CR, Shu CM. Complex thermal analysis and runaway reaction of 2,2′-azobis (isobutyronitrile)

using DSC, STA, VSP2, and GC/MS. J Loss Prev Process Ind. 2019;60:87–95.

63. Liu SH, Cao CR, Lin WC, Shu CM. Experimental and numerical simulation study of the thermal hazards of four azo compounds. J Hazard Mater. 2019;365:164–77.